

Quantum Spin Hall Insulators and Topological Rashba-splitting Edge States in Two-dimensional CX_3 ($X=Sb, Bi$)

Shan-Shan Wang^{†*}, Wencong Sun[†], and Shuai Dong[†]

[†]School of Physics, Southeast University, Nanjing 211189, China

S1. Electronic localized functions in CX_3 monolayer

The covalent bonding characters are evidenced by the presence of localized electrons between two nearest neighbor atoms, as clearly seen in the plot of ELF, Fig. S1.

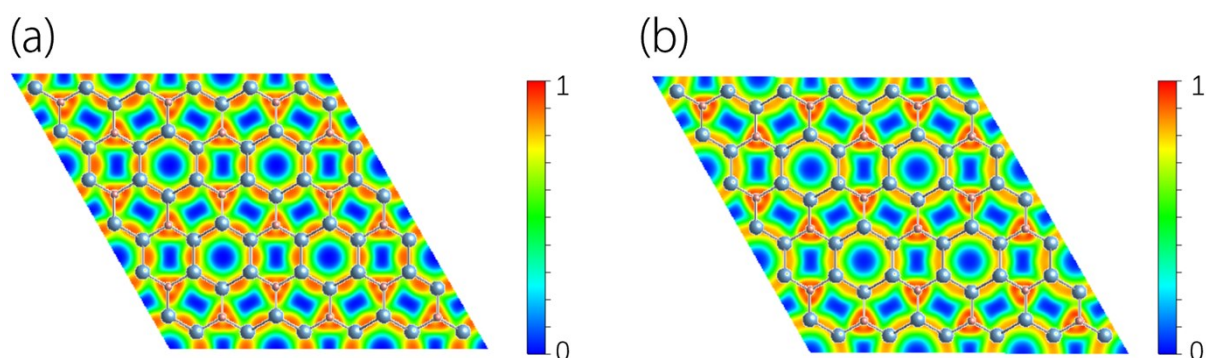


Figure S1. Electron localized function in CSb_3 (a) and CBi_3 (b) monolayers.

S2. Ab-Initio Molecular Dynamics Simulation of CX_3 ($X=Sb, Bi$)

We have performed the ab-initio Molecular Dynamics (AIMD) simulations to check the thermal stability of CX_3 monolayers. We take 4×4 supercell and the time step set to 1 fs. The snapshot of the systems at 300K after 9 ps are shown in the following Fig. S2. We see that the whole structure maintains its integrity, which validates the high structure stability.

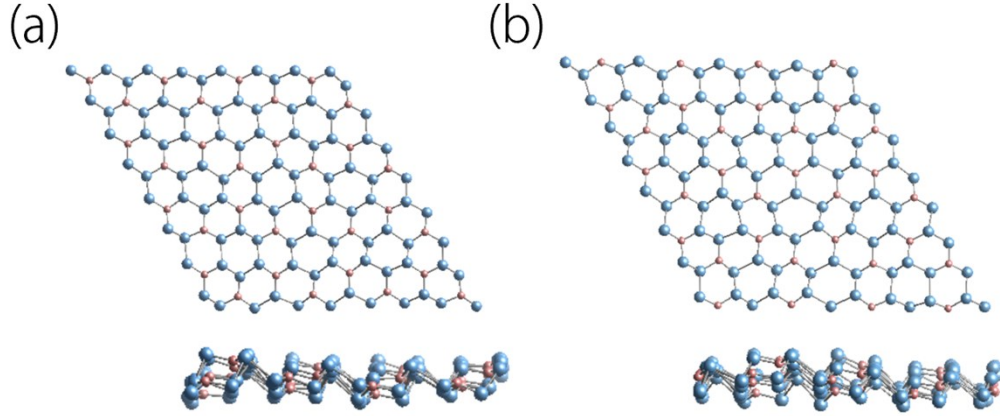


Figure S2. Snapshot of AIMD simulation result for CSb_3 (a) and CBi_3 (b) with 4×4 supercells.

S3. Wannier Charge Centers of CX_3 ($\text{X}=\text{Sb}, \text{Bi}$) with SOC.

The WCCs are calculated to determine the topological invariant of CX_3 monolayers, as shown in Fig. S3. The pattern of WCCs demonstrates that the WCCs can be crossed only one time by an arbitrary horizontal line, which doubly verified that $Z_2 = 1$.

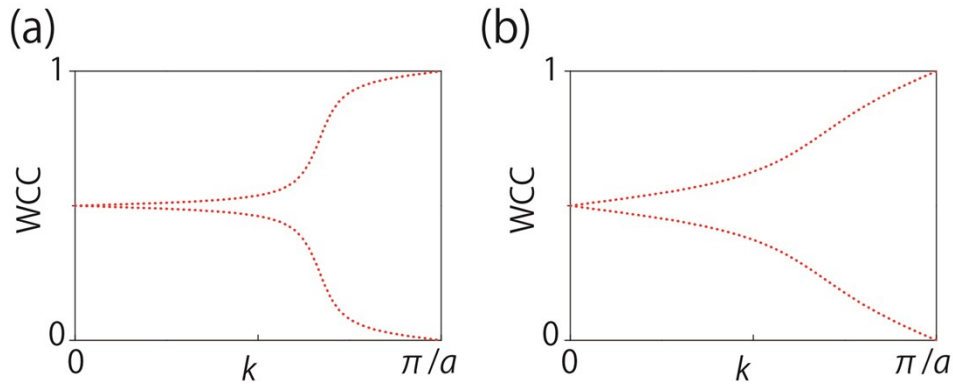


Figure S3. The pattern of WCCs for CSb_3 (a) and CBi_3 (b) monolayers.

S4. Convex Hull Diagram.

To estimate the thermodynamic stability. We construct the convex hull diagram of each binary systems by selecting four stable structures with the lowest free energy, as shown in Fig. S4. From the convex hull diagram, it is noted that CBi_3 and CSb_3 are thermodynamically stable.

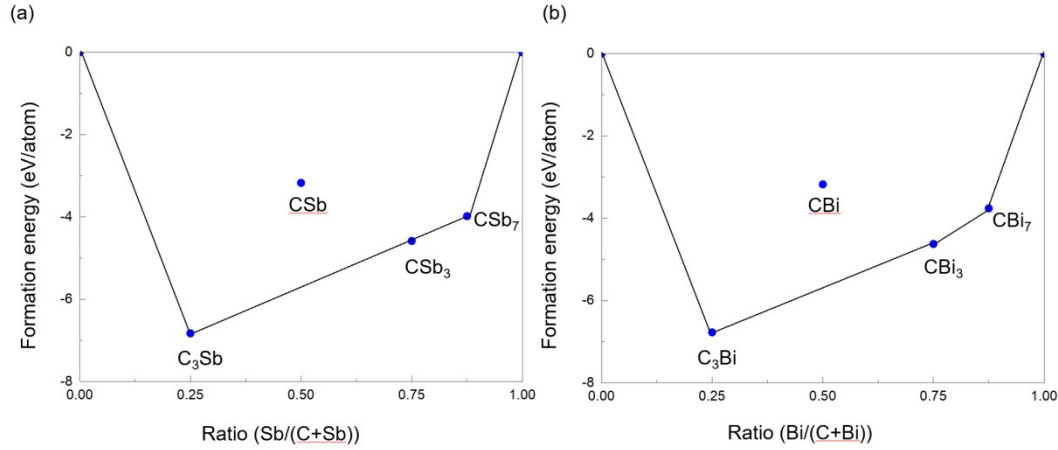


Fig. S4. Convex hull diagram of the C-X binary system at the PBE level. In each diagram, the x axis is composition ratio, and the y axis is the formation enthalpy in eV/atom relative to the ground states of the corresponding elemental allotropes.

S5. Potential Application in devices.

For device applications, it is in fact more convenient to work with nanostructures. In the revised version (Supplementary Material), we investigate the effect of a vertical electric field on the topological phase of CX_3 . Taking CSb_3 as an example, a vertical E-field can be used to tune the energy gap. It can induce a gap inversion and change the topological Z_2 character of CSb_3 , as shown in Fig. S5 (a). As a result, the system as a whole will undergo a field-induced topological phase transition between a QSH insulator and a trivial insulator.

The above findings enable an electrical control of the ON/OFF charge/spin conductance of helical edge states, which have significant implications on the design of QSH-based transistors. The E-field can be generated by the standard gating technique. To illustrate the feasibility of devices applications, we propose a topological field transistor (TFET) based on van der Waals heterostructures based on the detailed phase diagram shown in Fig. S5 (a). The schematic device is shown in Fig. S5 (b). Under ideal conditions, this device will support low-dissipation charge/spin transport in the ON state ($Z_2=1$) with spin polarized edge states. Applying an electric field will transform into a trivial insulator ($Z_2=0$) and turn the edge conduction OFF.

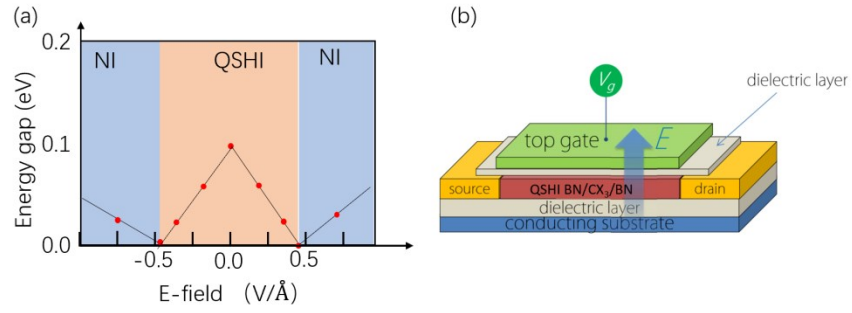


Fig. S5. Van der Waals heterostructured topological field effect transistor. (a) Topological phase diagram of CSb_3 monolayer as function of vertical electric field. The critical field strength is $\pm 0.48 \text{ V/\AA}$. (b) Schematic of van der Waals heterostructured field effect transistor. The central component is the van der Waals heterostructure of $\text{BN/CX}_3/\text{BN}$. Carriers are injected from source electrode and ejected from drain electrode. The ON/OFF switch is controlled by vertical electric field through the top and bottom gates.